Article

Not peer-reviewed version

Heritable Epigenetic Modification of BplAA9 Causes the Reversion Mutation of Leaf Shapes in *Betula pendula* ‘Dalecarlica’

Xingxing Zhang , Chenrui Gu , Jing Jiang , Guifeng Liu , Huiyu Li *

Posted Date: 14 November 2023

doi: 10.20944/preprints202311.0893.v1

Keywords: Betula pendula 'Dalecarlica'; DNA methylation; BplAA9

Article

Heritable Epigenetic Modification of *BpIAA9* Causes the Reversion Mutation of Leaf Shapes in *Betula pendula* 'Dalecarlica'

Xingxing Zhang, Chenrui Gu, Jing Jiang, Guifeng Liu and Huiyu Li *

State Key Laboratory of Tree Genetics and Breeding, Northeast Forestry University, No. 51, Hexing Road, Harbin, Heilongjiang 150040, China; zhanghanghang211@163.com (X.Z.); guchenrui@outlook.com (C.G.); jiangjing1960@126.com (J.J.); liuguifeng@126.com (G.L.)

* Correspondence: lihuiyu2020@nefu.edu.cn

Abstract: The European white birch, scientifically known as *Betula pendula*, and its variant, *B. pendula* 'Dalecarlica' are characterized by a serrated leaf margin that enhances their aesthetic appeal. However, the lobed leaf trait can undergo random and spontaneous reversion to the typical ovoid or cordate shape during asexual reproduction. Investigating and elucidating the molecular mechanisms underlying this unpredictable reversion mutation is essential for comprehending the birch leaf development process. In this research, we employed a non-lobed-leaf mutant derived from a lobed-leaf birch clone during plant tissue culture. We adopted a multi-omics approach, including whole-genome resequencing, transcriptome sequencing, and methylation profiling, to analyze and compare genomic variations and gene expression modifications. The study revealed that the 24 variant genes affected by 1464 SNP/InDel sites in the genome of the non-lobed-leaf mutant are not associated with leaf development. While the overall methylation level in the mutant's genome closely resembles that of the serrated-leaf birch, ten genes exhibit differential methylation accompanied by differential expression. Transcriptome sequencing demonstrated that the differentially downregulated genes in the mutant are significantly enriched in the GO:0009733 (response to auxin) and GO:0009734 (auxin-activated signaling) pathways. Validation through McrBC-PCR and qRT-PCR confirmed differential methylation and expression of *BpIAA9* in the reversion mutant. The elevated methylation level in the *BpIAA9* promoter leads to reduced expression, resulting in changes in the expression of auxin-responsive genes. This, in turn, leads to a transcriptional downregulation enrichment effect in auxin-related pathways in the reversion mutant, ultimately inhibiting the regulation of leaf veins by auxin during their development.

Keywords: *Betula pendula* 'Dalecarlica'; DNA methylation; *BpIAA9*

1. Introduction

Leaves are the primary organs responsible for photosynthesis and transpiration in plants[1]. Photosynthesis in leaves has a profound impact on a plant's growth, development, ecological benefits, and timber production[2,3]. Unlike smooth-edged leaves, serrated or lobed leaves provide a larger surface area and greater spatial expansiveness, making them advantageous for light absorption. This offers a competitive edge in light acquisition[4]. Additionally, these leaves possess enhanced aesthetic value.

The European birch, scientifically known as *Betula pendula*, is one of the most widely distributed tree species within the Birch genus, with extensive growth across the northern frigid regions of Eurasia. It holds significant practical value and developmental potential. This species exhibits strong cold resistance, has a deep-rooted system, thrives in poor soil conditions, and features an elegant stem structure, pristine bark, and gently cascading branches. As a result, it finds extensive utility in urban landscaping. The serrated-leaf birch, also known as *B.pendula* 'Dalecarlica' represents a variant of the European birch. Its leaves exhibit shallow serrations with elongated tips, prominent veins on the leaf undersides, significantly enlarged cross-sectional areas of internal mechanical transport tissues, and a more pronounced presence of epidermal trichomes on the leaf undersides[5].

 doi:10.20944/preprints202311.0893.v1

Birch is a monoecious species, but in the case of serrated-leaf birch, the male flowers are sterile. Consequently, it can only serve as the female parent for hybridization with European birch, leading to trait segregation in the offspring, with the majority displaying non-serrated leaves[6]. To ensure a higher proportion of plants in the next generation with consistent hereditary traits, plant tissue culture proves to be one of the most effective propagation methods. However, during asexual reproduction, serrated-leaf birch may undergo a random reversion mutation, resulting in the disappearance of serrations, and leaves reverting to their natural ovate or cordate shape. This phenomenon of reversion mutation can be reversed through treatment with 5-azacytidine (5-AzC), indicating a link between leaf morphological changes in serrated-leaf birch and epigenetics, particularly DNA methylation[7].

DNA methylation in eukaryotes can be classified into symmetric CG, CHG, and asymmetric CHH (with H representing A, T, or C) types. CHH methylation is a unique feature of plants and is established and maintained through the RNA-directed DNA methylation (RdDM) pathway[8]. These modifications play a controlled role in regulating the expression of neighboring genes[9,10]. Consequently, without altering the DNA sequence, they have a profound influence on leaf development and morphogenesis [11–14].

The morphological development of plant leaf primordia and young leaves is intricately regulated by the concentration of auxin, specifically Indole-3-Acetic Acid (IAA) [15]. Understanding leaf morphogenesis is critical for comprehending the formation and development mechanisms of nearly all lateral organs in plants, as these organs' development is governed by the concentration gradients of auxin [16–18]. The Auxin/Indole-3-Acetic Acid (Aux/IAA) gene family encodes short-lived nuclear proteins. In model organisms, these proteins possess specific structural domains that interact with Auxin Response Factors (ARF) and control the transcription of genes activated by ARFs, thus facilitating the transmission of auxin signals [19].

In previous studies, it was revealed that the *BpIAA*10 gene is involved in the development of birch leaves, the formation of dormant buds, the initiation and development of roots and stomata, and high growth. The specific auxin signaling pathways involved in *BpIAA*10 transcription factors were summarized, confirming that the birch AUX/IAA family proteins represented by *BpIAA*10 perform similar auxin signaling functions [20], However, no discernible impact of AUX/IAA on the serration of birch leaves has been observed.

This research was centered on an examination of two birch clones: one with serrated leaves and another without serrations, which was derived from the former during plant tissue culture. Employing a range of multi-omics techniques, including whole-genome resequencing, transcriptome sequencing, and methylation profiling, a comprehensive comparative analysis was carried out to elucidate the genomic variations and gene expression modifications between these two clones. The primary objective of this study was to unravel the underlying mechanism responsible for the formation of leaf serrations and to validate the pivotal differential genes involved in this process. The investigation revealed that alterations in DNA methylation levels and the expression of a gene belonging to the AUX/IAA family were the primary drivers of this mutation. This discovery offers valuable insights for refining the birch auxin signal transduction network and can serve as an invaluable resource and theoretical foundation for future birch breeding programs.

2. Materials and Methods

The serrated-leaf birch clone L72 (Figure 1) was obtained through tissue culture from a selected bud of a high-quality birch tree at the Northeast Forestry University's Birch Strengthening Seed Orchard. During the tissue culture process, adventitious shoots bearing ovate leaves were differentiated from callus tissue and designated as Y72 (Figure 1). All plantlets from the test tubes were subsequently transplanted into nursery pots (with a diameter of 18 cm and a depth of 20 cm, using a soil mixture composed of peat soil: vermiculite: perlite in a 3:1:1 ratio). They were then cultivated in the Birch Strengthening Seed Orchard, located at longitude 126.622615 E and latitude 45.716848 N.

 doi:10.20944/preprints202311.0893.v1

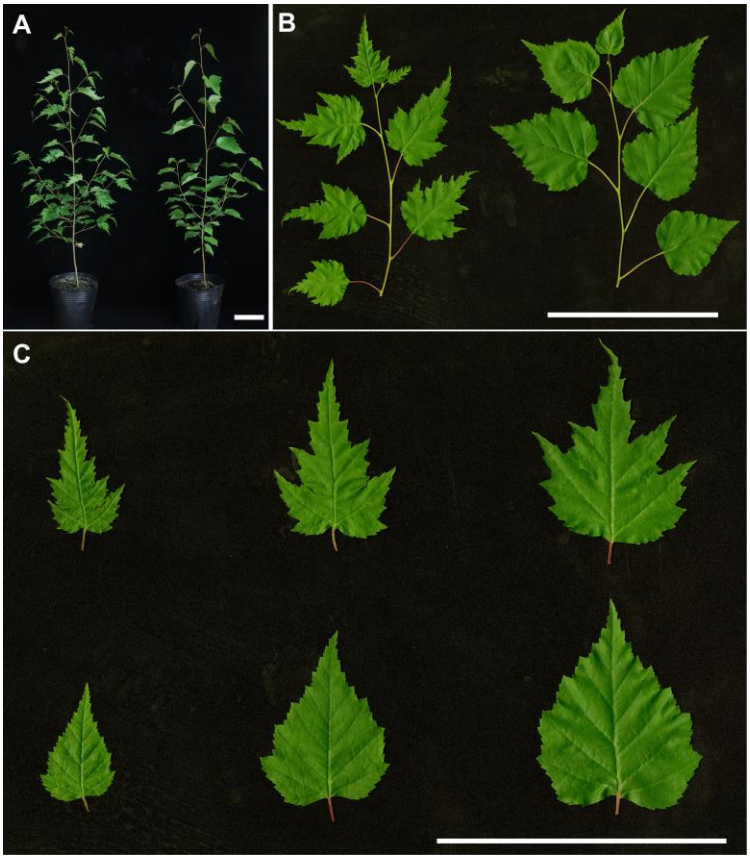

Figure 1. Serrated-Leaf Birch and Non-Lobed-Leaf Mutant. A-B: Seedlings and branches of *Betula pendula* 'Dalecarlica', identified as L72 (on the left), and its circular-leaf mutant Y72 (on the right).C: Leaves of L72 (at the top) and circular-leaf mutant Y72 (at the bottom), depicting the 1st (on the left), 2nd (in the middle), and 4th (on the right) leaves. Bar, 10 cm.

2.1. Tissue Culture of Serrated-Leaf Birch

The process of tissue culture for serrated-leaf birch involved the following steps: Collecting axillary buds from selected trees, washing them in distilled water for 12-24 hours, immersing them in 75% ethanol for 1 minute within a clean bench, rinsing with sterile water three times, disinfecting with 30% hydrogen peroxide for 10 minutes, and rinsing again with sterile water five times. After removing the bud scales, the white meristematic tissue was inoculated into differentiation medium (WPM + 0.8 mg/L 6-BA + 0.02 mg/L NAA + 0.5 mg/L GA_3 + 20 g/L sucrose + 5.65 g/L agar + 164 mg/L calcium nitrate). The wounded tissue developed into callus tissue and subsequently produced adventitious shoots. These shoots were transferred to the subculture medium (WPM + 0.8 mg/L 6-BA + 20 g/L sucrose + 5.65 g/L agar + 164 mg/L calcium nitrate), with fresh medium replaced every 25 days. Once the adventitious shoots grew into rootless plantlets, segments approximately 2 cm in height were cut and cultured on rooting medium (WPM + 0.4 mg/L IBA + 20 g/L sucrose + 5.65 g/L agar + 164 mg/L calcium nitrate) for 25-30 days until roots developed. Healthy, aseptic seedlings with well-developed roots, reaching a height of around 7 cm, were transplanted into nutrient pots containing a substrate mixture of peat soil: vermiculite: perlite = 3:1:1. These pots measured 10x10x10 cm and were placed in a greenhouse. Throughout the entire process, the cultivation conditions included a light intensity of 6000-8000 lux, a light/dark cycle of 16 hours/8 hours, an average temperature of 25°C, and a relative humidity of 60-70%.

2.2. Whole Genome Resequencing and Mutation Detection

On July 2, 2022, the fourth leaves of two-month-old serrated-leaf birch L72 and its circular-leaf mutant Y72 (Figure 1, C, right) underwent whole-genome resequencing. DNA extraction, library

 doi:10.20944/preprints202311.0893.v1

construction, and sequencing were conducted by Shanghai LingEn Biotechnology Co., Ltd., employing the Illumina NovaSeq 6000 platform. Following data filtering with fastp, clean reads were aligned to the reference genome using bwa[21], and the resulting files were sorted using samtools. Variant detection, encompassing SNPs and InDels, was executed using bcftools [22]. AnnoSNP was employed for the analysis of the impact of differential SNPs on coding genes, and the variant genes were annotated using eggnog-mapper.

2.3. Transcriptome (RNA-Seq) Sequencing and Analysis

On July 2, 2022, the fourth leaves of two-month-old serrated-leaf birch L72 and its round-leaf mutant Y72 (Figure 1, A, right) underwent transcriptome sequencing. RNA extraction, library preparation, sequencing, data quality control, and filtering were carried out by Shanghai LingEn Biotechnology Co., Ltd., using the Illumina Novaseq 6000 platform. The sequencing data were aligned to the birch reference genome (CoGe: 35079) using HISAT2, and gene expression was quantified using HTSeq. Differential gene analysis was performed using DESeq2.

2.4. Whole-Genome Bisulfite Sequencing

Whole-genome bisulfite sequencing (WGBS) was conducted on the fourth leaves of two-month-old *Betula pendula* L72 and its circular-leaf mutant Y72 on July 2, 2022 (Figure 1, C, right). DNA extraction, bisulfite treatment, library construction, and sequencing were carried out by Shanghai Ling En Biotechnology Co., Ltd., with a sequencing depth of 10X on the Illumina Novaseq 6000 platform. The sequencing data underwent quality control, filtering, and adapter trimming using fastp. The clean data were aligned to a reference genome using bsmap for methylation analysis, which included the identification of differentially methylated regions (DMRs) with a differential rate >0.33 and Fisher's exact test P-value <0.01 as the threshold. The results were visualized using the Integrative Genomics Viewer.

2.5. qRT-PCR

Total RNA was extracted from both the round leaves of *Betula pendula* and the fourth dissected leaf using the Plant RNA Extraction Kit (BioTeke Co. China). Subsequently, the RNA's integrity was evaluated by electrophoresis on a 1% agarose gel at 110V for 120 minutes. RNA purity was confirmed using a NanoPhotometer RP-Class spectrophotometer. The DNase-treated total RNA was reverse-transcribed into cDNA using a reverse transcription kit（ReverTra AceRqPCR RT Master Mix with gDNA Remover, Toyobo, Osaka, Japan), with primers consisting of a mixture of Oligo dT and random primers. The resulting cDNA was diluted tenfold and used as a template for qRT-PCR.

Primer design was facilitated by ApE and Primer 3 software (http://bioinfo.ut.ee/primer3-0.4.0/). These primers were used for relative quantitative PCR with the previously mentioned reverse-transcribed cDNA as the template. Each reaction contained 10 μL of Taq SYBR® Green qPCR Premix, 2 μL of cDNA template, 1 μL each of 10 μM gene-specific forward and reverse primers, and sterile water to reach a total volume of 20 μL. Real-time quantitative PCR was carried out using an ABI 7500 instrument (Applied Biosystems, Foster City, CA, USA) with the following program: 95°C for 30 seconds; 95°C for 15 seconds, followed by 60°C for 45 seconds for 45 cycles; 60°C for 1 minute; and a melt curve analysis from 95°C to 15 seconds. Each cDNA sample was analyzed in triplicate, and 18S rRNA and α-Tubulin were employed as internal reference genes. The relative expression level of the mRNA was calculated using the following formula: Relative mRNA expression level = 2^(-△△Ct).

2.6. McrBC-PCR

On May 8, 2023, leaf samples were collected and promptly preserved in liquid nitrogen. Total DNA extraction was carried out using a high-efficiency plant genomic DNA extraction kit (Trelief™ Hi-Pure Plant Genomic DNA Kit, Qiagen Biotech). The digested DNA was prepared by subjecting the DNA samples to McrBC digestion, utilizing the following reaction mixture for the enzyme-digested group: NEBuffer2 1 μL, 2 mg/mL rAlbumin 0.1 μL, 10 mM GTP 0.1 μL, 40 ng/μL DNA 5 μL,

Preprints (www.preprints.org) | NOT PEER-REVIEWED | Posted: 14 November 2023 doi:10.20944/preprints202311.0893.v1

McrBC 0.2 μL, and ultrapure water 3.6 μL. In the control group, all reagents necessary for the enzyme digestion reaction except McrBC were added to the DNA, and glycerol was used to reach the final volume (NEBuffer2 1 μL, 2 mg/mL rAlbumin 0.1 μL, 10 mM GTP 0.1 μL, 40 ng/μL DNA 5 μL, glycerol 0.2 μL, ultrapure water 3.6 μL). All reactions were conducted at 37°C for 12 hours. The digested DNA from both the enzyme-digested group and the control group served as templates for PCR amplification, utilizing the GoldenStarT6 DNA Polymerase Mix Ver.2 (TSE102, Qiagen, Beijing). The amplification products were visualized through GelRed staining and assessed by electrophoresis on a 2.5% agarose gel (120V, 400mA, 30 minutes). DNA bands were observed under ultraviolet imaging.

3. Results

3.1. Detection of Ovate Leaf Reversion Mutants

The results of the whole-genome resequencing analysis revealed that the serrated-leaf birch and ovate-leaf reversion mutant yielded 184.348244 million and 222.066586 million clean reads, respectively, both achieving a Q30 ratio exceeding 95%. A total of 6,625,724 SNP/InDel variations were identified. Fisher's test was conducted based on SNP/InDel sequencing depth for different genotypes, retaining 1,464 variant sites as differential SNP/InDel with $P < 0.05$. These differential SNPs were annotated using AnnoSNP, resulting in the identification of 24 variant genes. However, gene annotation revealed that none of these genes were associated with leaf morphogenesis (see Supplementary Table S1).

3.2. Enrichment of Differentially Expressed Genes in Reversion Mutants in Auxin Response and Auxin-Activated Signaling Pathways

RNA-Seq sequencing was performed separately on the leaves of the serrated-leaf birch L72 and the reversion mutant Y72, with each having three biological replicates. To ensure data reproducibility (see Supplementary Figure S1), one set of data (Y72-3) was excluded. The remaining five sets of sequencing data totaled 51.82 gigabases (Gb), all exhibiting Q30 ratios exceeding 96% and genome alignment rates exceeding 80%. DESeq2 was used to analyze differential gene expression, employing a threshold of $P < 0.05$ and $FC > 2$. This analysis identified a total of 1,009 differentially expressed genes, consisting of 392 upregulated genes and 617 downregulated genes (see Figure 1A). Enrichment analysis was performed separately for the upregulated and downregulated differentially expressed genes. Notably, only the downregulated gene set revealed potential pathways related to leaf margin morphology, particularly GO:0009733 (auxin response) and GO:0009734 (auxin-activated signaling) in the GO biological process enrichment analysis.

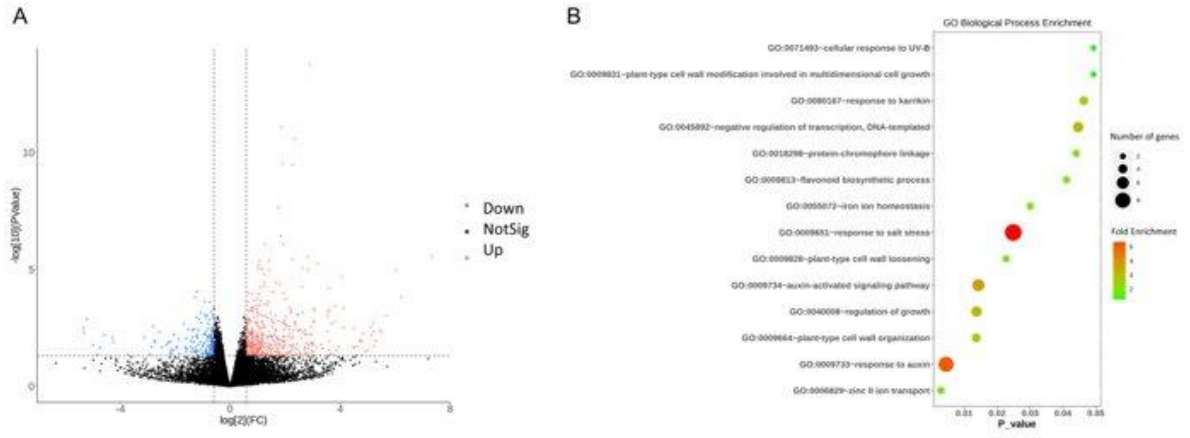

Figure 2. Transcriptome Sequencing Analysis. A, Volcano plot of differentially expressed genes. B, Enrichment results of downregulated differentially expressed genes in GO biological processes.

Preprints (www.preprints.org) | NOT PEER-REVIEWED | Posted: 14 November 2023 doi:10.20944/preprints202311.0893.v1

3.3. High Methylation in the Promoter Region of BpIAA9 in Mutant Plants with Downregulated Expression

Given the clonal reproduction of the round-leaf clone and the absence of genes related to leaf shape development, we conducted a comprehensive whole-genome methylation analysis to decipher the factors contributing to the variance in gene expression. Whole Genome Bisulfite Sequencing (WGBS) was performed on both sets of leaf samples, generating a total dataset of 48 Gbp with Q30 ratios exceeding 90%. Alignment using bsmap revealed alignment rates of over 60% to the reference genome.

We computed the average DNA methylation levels for genes and transposable elements (TEs) (see Figure 3). CpG DNA methylation levels were relatively low at gene transcription start and end sites but high in the gene bodies. In contrast, CHG and CHH methylation levels were highest at gene promoter and terminator regions. Within transposable elements, all three DNA methylation types displayed elevated levels both upstream and downstream of the main body. Notably, the round-leaf mutant exhibited increased CHH DNA methylation in gene promoter and terminator regions (see Figure 3, A). While the whole-genome methylation levels for all three DNA methylation types were higher in the round-leaf mutant compared to the serrated-leaf birch, these differences were not statistically significant ($P > 0.05$). These results suggest that the global DNA methylation levels in the round-leaf mutant have not significantly changed, but the transcription levels of specific genes may be influenced by variations in CHH methylation in their transcriptional regulatory regions.

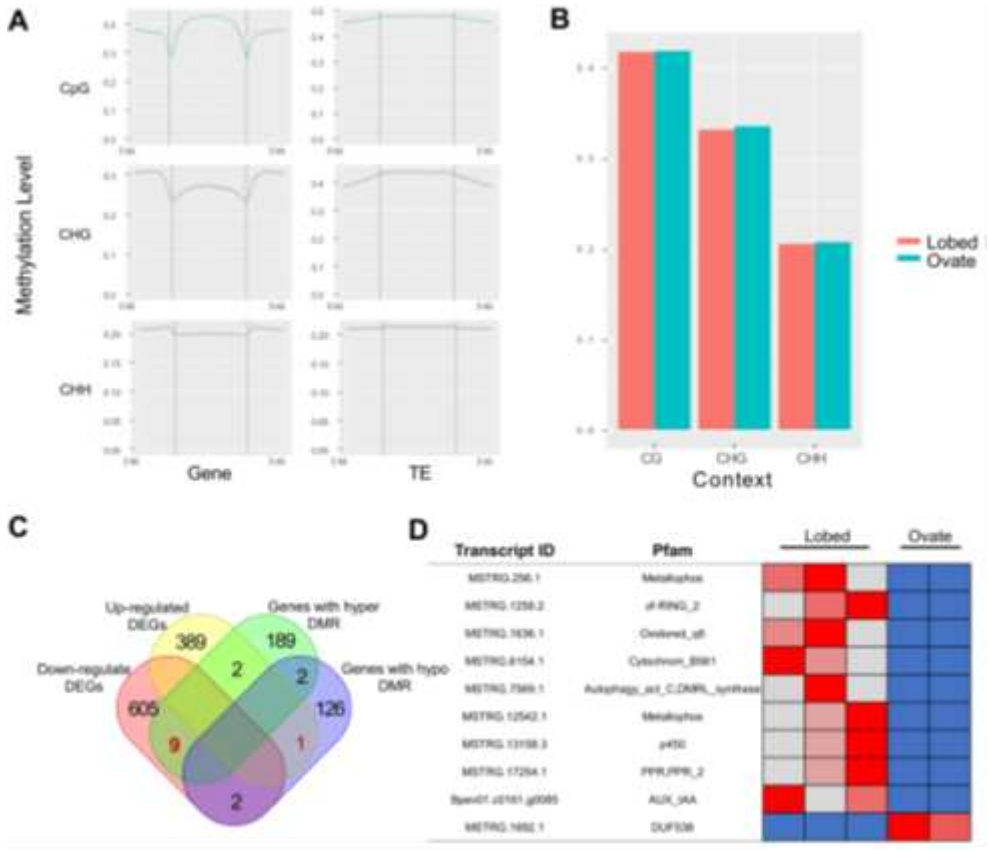

Figure 3. Whole-Genome Bisulfite Sequencing Results. A, Distribution of DNA methylation levels in gene and transposable element (TE) regions. B, Overall DNA methylation levels in the whole genome. C, Venn diagram depicting overlap between differentially methylated sites and differentially expressed genes. D, Heatmap of gene family annotations and expression levels of key genes.

Preprints (www.preprints.org) | NOT PEER-REVIEWED | Posted: 14 November 2023 doi:10.20944/preprints202311.0893.v1

A total of 3,053 differential methylation regions (DMRs) were identified from the whole-genome analysis. We conducted an analysis of the overlap between DMRs and differentially expressed genes. Among these, there were 9 downregulated genes associated with highly methylated regions, and 1 upregulated gene associated with a low-methylation region. Upon annotation, it was revealed that among these 10 genes, one belongs to the AUX_IAA transcription factor family, specifically *BpIAA9*[23], and its expression was significantly decreased in the round-leaf mutant ($P<0.01$) (Figure 3, C).

The visualization of WGBS results using IGV (see Figure 4, A) indicated that there were no significant changes in the CpG methylation level and CHG methylation level of *BpIAA9* in the round-leaf mutant. However, its promoter region exhibited a differential CHH methylation site (-950 to -1000 bp) in the round-leaf mutant, where DNA methylation levels were significantly higher compared to those in the silver birch. We examined the methylation level and transcription of *BpIAA9* in the apical buds, young leaves, and mature leaves of both the silver birch and the round-leaf mutant. McrBC results revealed that the methylation level of this site in the round-leaf mutant was slightly lower in the apical buds than in the silver birch, but significantly higher in the young and mature leaves (see Figure 4, B). qPCR results indicated that *BpIAA9* in the silver birch exhibited higher expression levels in young leaves, suggesting its involvement in leaf development (see Figure 4, C). In contrast, the transcription level of *BpIAA9* in the round-leaf mutant decreased, with significantly lower expression in young leaves compared to the silver birch ($P < 0.01$).

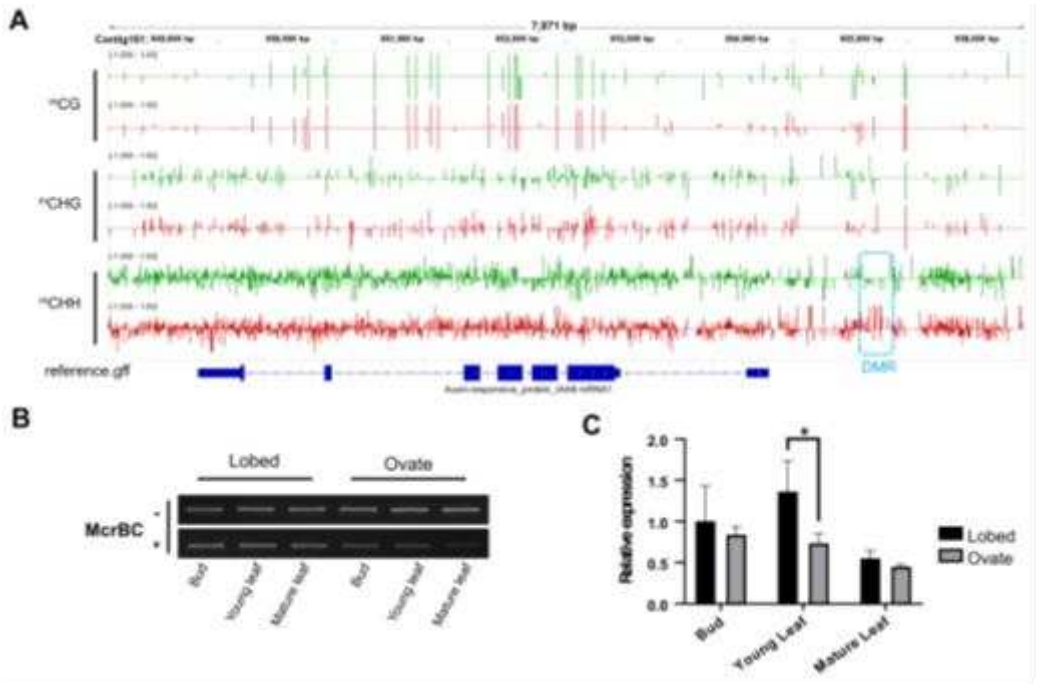

Figure 4. DNA Methylation and Transcription Levels of *BpIAA9*. A, IGV (Integrative Genomics Viewer) representation of DNA methylation levels of *BpIAA9* in serrated-leaf birch and non-lobed-leaf mutant. Green bars represent the methylation level of L72. Red bars represent the methylation level of Y72. B, McrBC-PCR results, where '-' indicates PCR product bands from undigested DNA templates and '+' indicates PCR product bands from DNA templates digested with McrBC. C, qPCR results of *BpIAA9* transcription levels, with '*' indicating statistically significant differences determined by t-test ($P < 0.05$).

 doi:10.20944/preprints202311.0893.v1

4. Discussion

Silver birch, *Betula pendula*, is a subspecies of European birch characterized by its serrated leaf margins. This trait is challenging to maintain during sexual reproduction and often spontaneously reverts to an ovate shape. It can also be induced to transform back into serrated leaves with the application of hormones or epigenetic mutagen 5-azacytidine (5AzC) [7]. These observations strongly suggest that the serrated leaf trait is under the control of epigenetic mechanisms. In our investigation of the round-leaf mutant, we identified 1464 differential single nucleotide polymorphisms (SNPs). These SNPs arise spontaneously during asexual reproduction, and yet, upon annotation, none of the 24 affected genes were found to be associated with leaf development. This further substantiates the notion that the serrated leaf trait is regulated by epigenetic factors rather than classical genetic traits.

Auxin plays a crucial role in regulating the morphogenesis of plant leaves [24-26]. This regulatory function involves various processes, including synthesis, transport, signal transduction, and degradation. In our transcriptomic analysis of the round-leaf mutant Y72, we observed a downregulation of genes associated with the Gene Ontology (GO) terms GO:0009733 (response to auxin) and GO:0009734 (auxin-activated signaling). This enrichment of genes related to auxin signaling and activation pathways suggests that in this mutant, there is an impediment in the gene expression responsible for auxin signal transduction and activation. While the concentration of auxin in different regions of silver birch leaves has been considered an important indicator[27], the response of target genes to these auxin signals has received relatively less attention. Our findings underscore the critical role of normal auxin signal transmission and gene activation in leaf development and morphogenesis.

Previous studies have revealed that a decrease in methylation modification in the promoter region of the *BpPIN*1 gene, a growth hormone transport protein, serves as a heritable epigenetic variation and a primary inducer of the fissured leaf trait in *Betula pendula* in both sexual and asexual reproduction processes[28]. However, in the circular leaf mutant Y72, we did not observe a significant restoration of methylation levels in *BpPIN*1 to the high levels found in the fissured leaf, as depicted in Figure 3, C to D. In comparison to fissured leaves, the global methylation levels across the genome of the circular leaf mutant showed no substantial changes in both genes and transposon elements, as shown in Figure 3, A to B. This suggests that the epigenetic maintenance function of this mutant remains unaltered, and its variation arises from random mutations in individual gene epigenetics. Through a combined analysis of differential methylation sites and differentially expressed genes, we identified a growth hormone signal transporter gene, *BpIAA*9. In birch, the transcription levels of AUX/IAA family transcription factors, such as *IAA*9, are influenced by various factors, including environmental conditions and endogenous growth hormone concentration[20]. These factors act by regulating downstream gene transcription in response to these signals. *IAA*9 functions as a transcriptional activator in processes influenced by growth hormones, such as root development and seedling growth. In the circular leaf mutant, the increased methylation levels in the promoter region of *BpIAA*9 led to decreased expression, impairing its ability to effectively transmit the growth hormone signal. In this situation of signal transmission inhibition, even if the methylation levels and expression of *BpPIN*1 remain at their original levels, the accumulated growth hormone concentration is insufficient to induce the fissured leaf trait.

CHH-type methylation is a plant-specific epigenetic modification, generally maintained through the RdDM pathway. In this model, the interaction between the CLASSY (CLSY) protein and SAWADEE Homolog 1 (SHH1) recruits RNA Polymerase IV (Pol IV) to silent heterochromatin regions, using these heterochromatic DNA segments as templates to synthesize short non-coding RNAs. These RNAs undergo a series of transformations to generate 24-nt small RNAs and form complexes with certain AGO proteins. AGO-sRNAs proceed along the RNA scaffold synthesized by RNA Polymerase V (Pol V), recruiting a series of protein complexes to enlist DNA methyltransferase 2 (DRM2) for catalyzing DNA methylation. Due to the positive feedback loop between CHH-type cytosine methylation and 24-nt small RNAs, once methylation is established, it can be heritably transmitted in both asexual and sexual reproductive processes[29].In this study, a highly methylated site within the *BpIAA*9 promoter was discovered. This methylation belongs to the CHH-type, and

Preprints (www.preprints.org) | NOT PEER-REVIEWED | Posted: 14 November 2023 doi:10.20944/preprints202311.0893.v1

McrBC-PCR analysis revealed that the level of methylation at this site is slightly lower in apical meristematic tissues but steadily increases in leaves as they grow and develop. This pattern could be attributed to the vigorous cell division in meristematic tissues, while this particular site lacks methylation in *Betula pendula.*

This research, employing various omics sequencing approaches, identified an epigenetic mutation site within the *BpIAA*9 promoter. The elevated methylation levels at this site led to a reduction in *BpIAA*9 expression. This disruption hampers the normal role of auxin in growth regulation and weakens the impact of abnormal auxin concentration gradients in leaf growth and development, eventually eliminating the fissured leaf trait (Figure 5). However, if mutations occur in other genes involved in auxin regulation, they could also induce the spontaneous reversion of *Betula pendula* from fissured to circular leaves. Therefore, in the asexual reproduction of *Betula pen21dula*, it is advisable to avoid factors that can induce changes in epigenetic modifications, including but not limited to temperature, salt, drought stress, and exposure to agents such as nicotinic acid and 5AzC. Further in-depth research on the genetic transformation and methylation variation mechanisms of *BpIAA*9 is warranted in future studies.

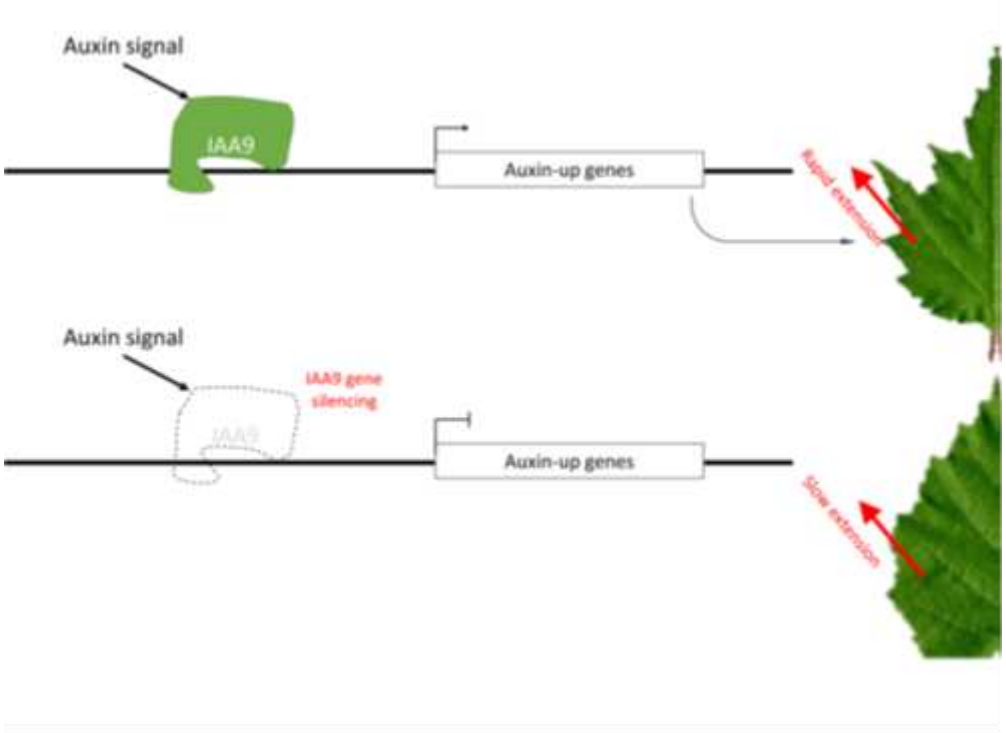

Figure 5. A schematic illustration of the proposed mechanism underlying the role of DNA methylation in altering the shape of birch leaves. The high methylation in the promoter region leads to decreased expression of *BpIAA*9 at the edge of the leaf primordia, thereby blocking the normal function of auxin, resulting in the elimination of the lobed leaf trait and the restoration of a round leaf shape.

Supplementary Table S1. Annotation of Coding Variant Genes.

GeneID	Description	PFAMs
Bpev01.c0042.g0072	LRR receptor-like serine threonine-protein kinase At3g47570	LRRNT_2,LRR_1,LRR_8,Pkinase,Pkinase_Tyr
Bpev01.c2373.g0003	Ribonuclease H protein	Exo_endo_phos_2,RVT_1,RVT_3,zf-RVT

 doi:10.20944/preprints202311.0893.v1

Bpev01.c0051.g0044	zinc finger CCCH domain-containing protein	CwfJ_C_1,CwfJ_C_2,zf-CCCH
Bpev01.c0056.g0001	Non-functional NADPH-dependent codeinone reductase 2-like	Aldo_ket_red
Bpev01.c0106.g0013	Belongs to the cyclin family	Cyclin_C,Cyclin_N
Bpev01.c0148.g0013	Homeobox protein knotted-1-like	ELK,Homeobox_KN,KNOX1,KNOX2
Bpev01.c0159.g0037	Lignin degradation and detoxification of lignin-derived products	Cu-oxidase,Cu-oxidase_2,Cu-oxidase_3
Bpev01.c0213.g0030	receptor	PA,cEGF
Bpev01.c0261.g0047	Protein AUXIN SIGNALING F-BOX	F-box-like,LRR_6
Bpev01.c0418.g0001	Probably involved in the RNA silencing pathway and required for the generation of small interfering RNAs (siRNAs)	RdRP
Bpev01.c0547.g0018	wall-associated receptor kinase-like	EGF_CA,GUB_WAK_bind,Pkinase,Pkinase_Tyr,WAK
Bpev01.c0665.g0008	Zinc phosphodiesterase ELAC protein	Lactamase_B_2,Lactamase_B_4
Bpev01.c0727.g0025	protein serine/threonine kinase activity	Malectin_like,Pkinase_Tyr
Bpev01.c1122.g0007	Belongs to the universal ribosomal protein uL23 family	Ribosomal_L23,Ribosomal_L23eN
Bpev01.c1136.g0001	ribonuclease H protein	RVT_1,RVT_3,zf-RVT
Bpev01.c1152.g0017	Belongs to the glycosyl hydrolase 17 family	Glyco_hydro_17

Preprints (www.preprints.org) | NOT PEER-REVIEWED | Posted: 14 November 2023 doi:10.20944/preprints202311.0893.v1

Bpev01.c1155.g0004	Asparagine-specific endopeptidase involved in the processing of vacuolar seed protein precursors into the mature forms	Peptidase_C13
Bpev01.c1170.g0014	Protein of unknown function (DUF620)	DUF620
Bpev01.c1242.g0006	Pentatricopeptide repeat-containing protein	PPR,PPR_2
Bpev01.c1533.g0002	ribonuclease H protein	RVT_1,RVT_3,zf-RVT
Bpev01.c1748.g0004	rRNA processing/ribosome biogenesis	RIX1
Bpev01.c2125.g0002	G-type lectin S-receptor-like serine threonine-protein kinase	B_lectin,DUF3403,GUB_WAK_bind,PAN_2,Pkinase_Tyr,S_locus_glycop
Bpev01.c1039.g0006	Unknown	Unknown
Bpev01.c0575.g0017	Unknown	Unknown

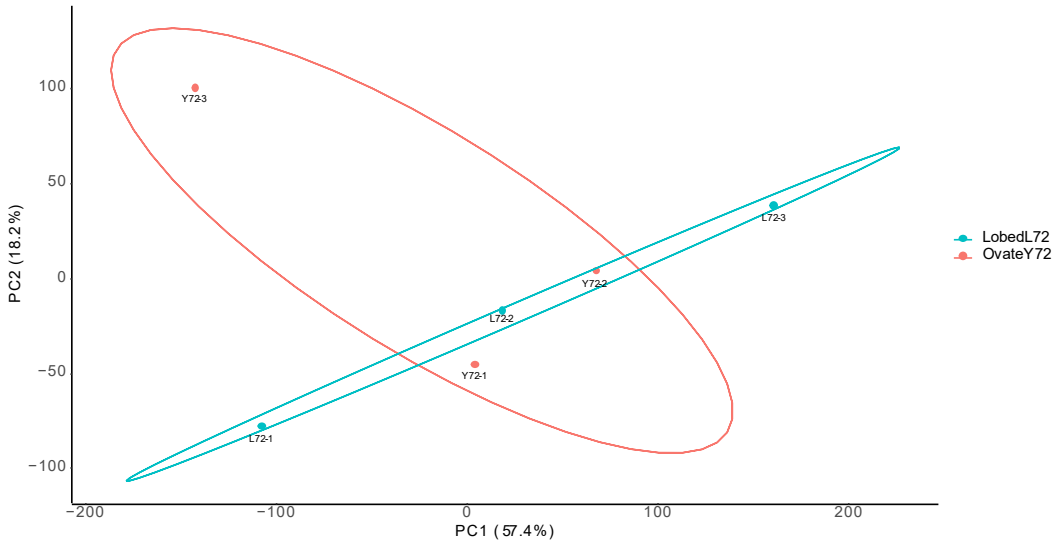

Supplementary Figure S1. The principal component analysis results for biological replicates of transcriptome sequencing.

Supplementary Materials: The following supporting information can be downloaded at the website of this paper posted on Preprints.org, Table S1: Annotation of Coding Variant Genes; Figure S1: The principal component analysis results for biological replicates of transcriptome sequencing.

Author Contributions: Conceptualization, X.Z. and C.G.; methodology, H.L.; software, X.Z. and C.G.; validation, X.Z. and C.G.; formal analysis, C.G.; investigation, X.Z. and C.G.; resources, X.Z., C.G. and H.L.; data curation, C.G.; writing—original draft preparation, X.Z. and C.G.; writing—review and editing, X.Z. and H.L.; visualization, X.Z.; supervision, H.L., G.L. and J.J.; project administration, H.L.; funding acquisition, H.L., G.L. and J.J. All authors have read and agreed to the published version of the manuscript.

Funding: This research was funded by the National Key R&D Program Sub-Project (2021YFD2200105) and the "Heilongjiang Touyan Innovation Team Program (Tree Genetics and Breeding Innovation Team)" Basic Research Fund (2021YFD2200304).

Data Availability Statement: The original contributions presented in the study are publicly available. These data can be found here: NGDC, Bio Project: PRJCA021170.

Conflicts of Interest: The authors declare no conflict of interest.

References

1. Qu, M.; Hamdani, S.; Li, W. Rapid stomatal response to fluctuating light: an under-explored mechanism to improve drought tolerance in rice. *Funct Plant Biol* **2016**, *43(8)*, 727–738.
2. Zhao, W.; Liu, L.; Shen, Q. Effects of water stress on photosynthesis, yield, and water use efficiency in winter wheat. *Water* **2020**, *12*, 2127.
3. Xia, J.B.; Zhang, G.C.; Wang, R.R. Effect of soil water availability on photosynthesis in Ziziphus jujuba var. spinosus in a sand habitat formed from seashells: Comparison of four models. *Photosynthetica* **2014**, *52(2)*, 253–261.
4. Ou, G.; Bei, L.; Zhang, J. Effects of the Leaf Shape and Growth Posture on Light Use Efficiency of Cassava (in Chinese). *MPB* **2023**, 1–21.
5. Qu, C.; Bian, X.; Jiang, J. Leaf morphological characteristics and related gene expression characteristic analysis in *Betula pendula* 'Dalecarlica' and *Betula pendula* (in Chinese). *Journal of Beijing Forestry University* **2017**, *39(08)*, 9–16.
6. Tian, S.; Ma, Q.; Wang, Y. Segregation of Seed Vigor and Leaf Traits in Hybrid Progenies of *Betula pendula* 'Purple Rain' and *Betula pendula* 'Dplecprlicp' (in Chinese). Forest Research. **2019**, *32(03)*, 40–48.
7. Mashkina, O.S.; Tabatskaya, T.M. Morphogenesis of a Dissected Birch Leaf in vitro Culture. *Russ. J. Dev. Biol.* **2020**, *51(6)*, 397–409.
8. Zhang, H.; Lang, Z.; Zhu, J. Dynamics and function of DNA methylation in plants. Nature reviews. *J. Mol. Cell Biol.* **2018**, *19(8)*, 489–506.
9. Zhang, X.; Yazaki, J.; Sundaresan, A. Genome-wide high-resolution mapping and functional analysis of DNA methylation in arabidopsis. *Cell*. **2006**, *126(6)*, 1189–1201.
10. Zhang, H.; Zhu, J. RNA-directed DNA methylation. *Curr. Opin. Plant Biol.* **2011**, *14(2)*, 142–147.
11. Kakutani, T.; Jeddeloh, J. A.; Richards, E. J. Characterization of an Arabidopsis thaliana DNA hypomethylation mutant. *Nucleic Acids Res.* **1995**, *23(1)*, 130–137.
12. Paula, J.M.D.; Pinto-Maglio, C.A.F.; Pinto, L. R. Morphological analysis and DNA methylation in Conyza bonariensis L. cronquist (Asteraceae) phenotypes. *Bragantia* **2017**, *76(4)*, 480–491.
13. Finnegan, E. J.; Peacock, W. J.; Dennis, E. S. Reduced DNA methylation in Arabidopsis thaliana results in abnormal plant development. *Proc. Natl. Acad. Sci. U.S.A.* **1996**, *93(16)*, 8449–8454.
14. Ci, D.; Song, Y.; Du, Q. Variation in genomic methylation in natural populations of Populus simonii is associated with leaf shape and photosynthetic traits. *J. Exp. Bot.* **2016**, *67(3)*, 723–737.
15. Yanagisawa, M.; Poitout, A.; Otegui, M. S. Arabidopsis vascular complexity and connectivity controls PIN-FORMED1 dynamics and lateral vein patterning during embryogenesis. *Development (Cambridge)*. **2021**, *148(14)*.
16. Shen, J.; Zhang, Y.; Ge, D. CsBRC1 inhibits axillary bud outgrowth by directly repressing the auxin efflux carrier CsPIN3 in cucumber. *PNAS* **2019**, *116(34)*, 17105–17114.
17. Zhu, M.; Chen, W.; Mirabet, V. Robust organ size requires robust timing of initiation orchestrated by focused auxin and cytokinin signalling. *Nat Plants.* **2020**, *6(6)*, 686–698.
18. Lv, X.; Zhang, M.; Li, X. Transcriptome Profiles Reveal the Crucial Roles of Auxin and Cytokinin in the "Shoot Branching" of Cremastra appendiculata. *Int. J. Mol. Sci.* **2018**, *19(11)*, 3354.
19. Luo, J.; Zhou, J.; Zhang, J. Aux/IAA Gene Family in Plants: Molecular Structure, Regulation, and Function. *Int. J. Mol. Sci.* **2018**, *19(1)*, 259.

20. Xu, W.; Han, R.; Xu, S. Expression of *BpIAA*10 from *Betula platyphylla* (birch) is differentially regulated by different hormones and light intensities. *Plant Cell Tiss. Org.* **2018**, *132(2)*, 371–381.
21. Li, H.; Durbin, R. Fast and accurate long-read alignment with Burrows-Wheeler transform. *IJB* **2010**, *26(5)*, 589–595.
22. Danecek, P.; Bonfield, J. K.; Liddle, J. Twelve years of SAMtools and BCFtools. *Gigascience* **2021**, *10(2)*.
23. Xu, W.; Chen, S.; Jiang, J. Expression profiling of the *BpIAA* gene family and the determination of IAA levels in *Betula platyphylla* tetraploids. *JFR.* **2019**, *30(3)*, 855–867.
24. Xiong, Y.; Wu, B.; Du, F. A crosstalk between auxin and brassinosteroid regulates leaf shape by modulating growth anisotropy. *Molecular plant* **2021**, *14(6)*, 949–962.
25. Ben-Gera, H.; Ori, N. Auxin and LANCEOLATE affect leaf shape in tomato via different developmental processes. *Plant Signaling & Behavior* **2012**, *7*, 1255–1257.
26. Nikolov, L.A.; Runions, A.; Das Gupta, M. Chapter Five – Leaf development and evolution. *Current Topics in Developmental Biology*; Grossniklaus, Ueli; Academic Press: Grossniklaus U, USA, 2019; 131, pp. 109–139.
27. Qu, C.; Bian, X.; Han, R. Expression of *BpPIN* is associated with IAA levels and the formation of lobed leaves in *Betula pendula* 'Dalecartica'. *JFR.* **2020**, *31(1)*, 87–97.
28. Gu, C.; Han, R.; Liu, C. Heritable epigenetic modification of *BpPIN*1 is associated with leaf shapes in *Betula pendula*. *Tree Physiol.* **2023**, *43(10)*,1811–1824.
29. Matzke, M.A.; Mosher, R.A. RNA-directed DNA methylation: an epigenetic pathway of increasing complexity. *Nat Rev Genet*. **2014**, *15(6)*, 394–408.